Biophysical Chemistry 153 (2010) 83–96

Contents lists available at ScienceDirect

Biophysical Chemistry

journal homepage: http://www.elsevier.com/locate/biophyschem

A modified model for translocation events of processive nucleotide and repeat additions by the recombinant telomerase

Ping Xie *

Key Laboratory of Soft Matter Physics and Beijing National Laboratory for Condensed Matter Physics, Institute of Physics, Chinese Academy of Sciences, Beijing 100190, China

ARTICLE INFO

Article history:
Received 26 August 2010
Received in revised form 11 October 2010
Accepted 12 October 2010
Available online 16 October 2010

Keywords:
Telomere
Nucleotide addition processivity
Repeat addition processivity
Molecular motor
Model

ABSTRACT

Telomerase is a unique reverse transcriptase that extends the single-stranded 3′ overhangs of telomeres by copying a short template sequence within the integral RNA component of the enzyme. It shows processive nucleotide and repeat addition activities, which are realized via two types of movements: translocation of the DNA:RNA hybrid away from the active site following each nucleotide addition and translocation of the 3′ end of the DNA primer relative to the RNA template after each round of repeat synthesis. Here, a model is presented to describe these two types of translocation events by the recombinant *Tetrahymena* telomerase, via the modification of the model that has been proposed recently. Using the present model, the dynamics of the dissociation of the DNA primer from the telomerase and the dynamics of the disruption of the DNA:RNA hybrid and then repositioning of the product 3′ end to the beginning of the template are studied quantitatively. Their effects on the repeat addition processivity are theoretically studied. The theoretical results are in agreement with the available experimental data.

1. Introduction

Telomerase is a specialized ribonucleoprotein (RNP) complex that uses an intrinsic RNA to template the synthesis of telomeres onto the 3′ ends of linear eukaryotic chromosomes [1–5]. The telomerase RNP functions as a multisubunit holoenzyme that contains an RNA component (telomerase RNA), a catalytic protein component telomerase reverse transcriptase (TERT) and other associated proteins [6]. The telomerase activity was discovered firstly in the ciliate *Tetrahymena thermophila* by Greider and Blackburn in 1985 [1] and subsequently in many other eukaryotes [7–16]. *Tetrahymena* telomerase RNA is a 159 nucleotide transcript, which contains the sequence 3′-AACCCCAAC-5′ that serves as a template for synthesis of the telomeric repeat TTGGGG [17]. Immediately located 5′ of the template is a template boundary element (TBE) and 3′ of the template is a template recognition element (TRE) [18,19]. Besides of these template-adjacent elements, pseudoknot III and stem-loop IV are also shown to play important roles in telomerase function [18,20–22]. The TERT protein contains polymerase active site motifs shared among all reverse transcriptases [23] as well as unique N-terminal extension (TEN) and C-terminal extension that harbor both phylogenetically conserved and variable motifs [24]. A recently solved structure of *Tribolium castaneum* telomerase catalytic subunit TERT revealed that it consists of a RNA-binding domain (TRBD), a putative thumb domain and a reverse transcriptase (RT) domain that includes a palm subdomain and a finger subdomain that is simply called “fingers” [25]. The RT domain is most similar to those of HIV RT, DNA polymerase (DNAP) and RNA polymerase (RNAP). Of the accessory proteins, p65 has been shown to form a complex with telomerase RNA, playing the role in assembly of telomerase RNP [26–28].

Compared to other polymerase enzymes such as DNAP, retroviral RT and RNAP, the most peculiar feature of the telomerase is its ability to synthesize long stretches of a DNA primer by using the short template sequence within telomerase RNA [2,17,29,30]. This requires that the telomerase is able to carry out two types of translocation events: (i) translocation of the active site along the template after each nucleotide incorporation (nucleotide addition processivity) and (ii) the disruption of the DNA:RNA hybrid and then repositioning of the product at the 3′ end to the beginning of the template after each round of repeat synthesis (repeat addition processivity). It has been shown that the *in vitro* recombinant telomerases that are composed of only the two subunits telomerase RNA and TERT suffice to give the telomerase activity [31,32], but the recombinant *Tetrahymena* enzyme demonstrates a more limited repeat addition processivity than the endogenous one [33].

Recently, we have presented a model to describe these two types of translocation events by the recombinant *Tetrahymena* telomerase [34]. In the model, the forward translocation of the active site along the template during the processive nucleotide addition is rectified through the incorporation of a matched nucleotide complementary to

* Tel.: +86 10 82649387; fax: +86 10 82640224.
E-mail address: pxie@aphy.iphy.ac.cn.

0301-4622/$ – see front matter © 2010 Elsevier B.V. All rights reserved.
doi:10.1016/j.bpc.2010.10.007

the template unpaired base, via the Brownian ratchet mechanism, as proposed previously for DNAP [35]. After each round of repeat synthesis, the unpairing of the DNA:RNA hybrid and then repositioning of the product at the 3′-end on the template are caused by a force acting on the primer. The force results from the unfolding of stem III pseudoknot that is automatically induced by the rotation of the fingers together with stem IV loop toward the nucleotide-bound active site. However, before the incorporation of the nucleotide paired with the last base on the template, the force mainly acts on the template rather than on the primer and, thus, the DNA:RNA hybrid cannot be disrupted.

In this work, we present a modified model based on the previous one. Several important factors, which affect the nucleotide addition and repeat addition processivities but have not been considered in the previous model, are incorporated into and considered in the modified model. We add the interaction of the DNA primer with the DNA-binding site adjacent to the 3′ terminus of the RNA template. The dissociation of the primer from the telomerase is taken into account. We study the effect of the elastic potential change resulting from the deviation of the RT domain from its equilibrium position relative to the TEN and TRBD domains on the repeat addition processivity. The theoretical results based on the modified model are in agreement with the available experimental data.

2. Model

Our modified model is constructed based on the following four basic hypotheses. Hypotheses I and II are the same as those described in the previous work [34], while Hypotheses III and IV are modified on the previous ones.

2.1. Four hypotheses

2.1.1. Hypothesis I

In the RT domain of TERT, there exists an ssRNA-binding site A adjacent to the active site. The binding site A has an affinity for the unpaired base (or the sugar-phosphate backbone of the unpaired base) on the template in the RNA component.

This hypothesis is the same as that stated in the previous work [34]. The experimental evidence for supporting the hypothesis is described as follows. The co-immunoprecipitation assay showed that, besides other regions such as TBE element and TRE element in the RNA component, the template region of *Tetrahymena* telomerase is also important for optimal TERT binding [20]. From the available structure of the *T. castaneum* telomerase catalytic subunit TERT, it is implicated that the active site is located in the palm subdomain and adjacent to the finger subdomain [25]. Thus, the binding site *A*, which is adjacent to the active site, should be also located in the RT domain. Note that the hypothesis is similar to that adopted in other polymerase enzymes. For example, in replicative DNAP and retroviral RT, it was also hypothesized that there exists an ssDNA-binding site in the vicinity of the active site that has an affinity for the unpaired base (or the sugar-phosphate backbone of the unpaired base) on template DNA [35,36]. Comments on the affinity of site *A* for the template in telomerase will be given later (see Section 3.3.1).

In replicative DNAP and retroviral RT [35,36], the interaction of site *A* with ssDNA can be used to explain the induced-fit mechanism. Similarly, we have the following anticipation for the telomerase. The interaction of the site *A* with an unpaired base on the template RNA induces the conformational change in residues in the vicinity of the active site that is adjacent to the site *A*. This unpaired-base-related conformational change thus results in the active site having a much higher affinity for the structurally compatible nucleotide than structurally incompatible nucleotides, resulting in the high-fidelity nucleotide incorporation.

2.1.2. Hypothesis II

The binding of a nucleotide to the active site induces the finger subdomain to rotate towards the active site. Stem IV is bound to the finger subdomain of TERT. Thus, accompanying the inward rotation of the fingers upon a nucleotide binding, stem IV loop is also rotated—from its equilibrium position that is away from the active site—towards the active site. The closed conformation of the fingers and stem IV activates the nucleotide incorporation. When the active site is nucleotide-free, the fingers together with stem IV loop rotate outwards, away from the active site. The open conformation of fingers and stem IV opens the active site for the nucleotide to slide into.

This hypothesis is the same as that stated in the previous work [34]. The experimental evidence for supporting the hypothesis is described as follows. The available structure of the *T. castaneum* telomerase catalytic subunit TERT showed that telomerase finger and palm subdomains are most similar to those of B-family DNAP, retroviral RT and viral RNAP. On the other hand, available structures showed that, in bacteriophage T7 DNAP [37,38] and HIV RT [39], the nucleotide binding to (releasing from) the active site induces the rotation of the finger subdomain from open (closed) to closed (open) conformation, with the nucleotide being able to bind to the active site in the open-finger conformation while the closed-finger conformation activating the chemical reaction of nucleotide incorporation. In single-subunit phage T7 RNAP, the nucleotide binding (releasing) induces the rotation of an α helix, termed the O helix, from open (closed) conformation to closed (open) conformation, with the nucleotide being able to bind to the active site in the open conformation while the closed conformation activating the nucleotide incorporation [40,41]. Furthermore, biochemical data for telomerase showed that the telomerase RNP with RNA lacking stem IV exhibits weak nucleotide addition activity [20–22]; stem IV loop in the RNA component binds TERT directly [20].

The hypothesis implies that, in the closed conformation, both the fingers of TERT and the stem IV of telomerase RNA contribute to the activation of nucleotide incorporation. In other words, without either the fingers or the stem IV, the nucleotide addition activity is reduced greatly, which is consistent with the available experimental results [20–22]. This feature is slightly different from that in DNAP, retroviral RT and RNAP, wherein the fingers alone can effectively activate the nucleotide incorporation. The hypothesis that stem IV loop in the RNA component is bound to the finger subdomain of TERT is consistent with the experimental results showing that stem IV binds TERT directly [20]. Although recent evidence indicated that stem-loop IV interacts with the TRBD [42], from the available structure of *T. thermophila* TRBD [43] and the structure of the full-length *T. castaneum* telomerase [25] we infer that the hypothesis that stem-loop IV binds to the fingers could be reconciled with this recent evidence (see Section S1 in the Appendix).

2.1.3. Hypothesis III

The 3′ end of the DNA primer is bound on the template region of the RNA via forming the DNA:RNA hybrid. The 5′ end is bound in an anchor site that has specificity for telomeric sequence or a G-rich sequence. The DNA base opposite template base A51 and the next adjacent 5′ DNA base are bound to a site located in TEN domain.

This three-site hypothesis for the interaction between telomerase and DNA primer is the modified one based on the two-site hypothesis stated in the previous work [34]. As proposed in the literature [44,45], the two-site hypothesis only considers the existence of the anchor site and the formation of the DNA:RNA hybrid at the 3′ end of the primer. Here, besides of these two sites, we also include the site, called primer alignment site (PAS), that interacts with the DNA base opposite template base A51 and the next adjacent 5′ DNA base. The hypothesis of the existence of the PAS is consistent with the experimental data of Baran et al. [46], Romi et al. [47] and Jacobs et al. [48]. Based on these

experiments and the experiment of Finger and Bryan [49], it appears that the PAS is composed of residues Trp187 and Phe178 in *Tetrahymena* TEN domain that interact with the DNA base opposite template base A51 and the next adjacent 5′ DNA base, respectively, while the anchor site is composed of residue Gln168 in TEN domain and residues in other domains such as TRBD and C-terminal domain.

2.1.4. Hypothesis IV

The connection residues between domains (the TEN and TRBD domains), which contain the anchor site and PAS, and the RT domain, which contains the binding site A and the active site, are considered to behave elastically when the connection residues are stretched. Moreover, there exists an affinity between the TEN and RT domains, making one domain stabilized in the equilibrium position (with relaxed connection residues) relative to the other one.

Here, we add the presence of an affinity between the TEN and RT domains, which has been overlooked in the previous work [34]. The hypothesis that the active site can be movable relative to the PAS is consistent with the experimental evidence of Romi et al. [47]. The ability of the RT domain to move relative to the TEN and TRBD domains is also consistent with the suggestion of Romi et al. [47]. Based on the available structure of *T. thermophila* TRBD [43] and on the comparison with the structure of the full-length *T. castaneum* telomerase [25], the displacement of the RT domain relative to TRBD in *thermophila* telomerase could be accommodated by the three extended loops linking the two halves of the TRBD (see Section S1 in the Appendix). As our model will show (see below), the presence of the interaction between the TEN and RT domains is consistent with the experiment of Zaug et al. [50] showing that *Tetrahymena* telomerases by mutating Leu14 in the TEN domain retain nucleotide addition activity and anchor-site function but lose repeat addition processivity.

2.2. Mechanism of processive nucleotide addition

Based on the four hypotheses, the modified model for processive nucleotide and repeat additions by the recombinant telomerase is schematically shown in Fig. 1. We use *T. thermophila* telomerase as an example to illustrate the model, where the telomerase RNA is a 159-nucleotide transcript and the template region (3′-AACCCCAAC-5′) is from nucleotides 51 to 43 [17].

We begin with the binding site *A*, in the equilibrium position relative to the TEN and TRBD domains, binding the unpaired base 48 on the template region of RNA (Fig. 1a), where the PAS is bound to the DNA base opposite template base A51 and the next adjacent 5′ DNA base, bases 49–51 of template RNA are bound to the 3′ end of the primer through Watson–Crick base-pairing, and the anchor site is bound to the upstream sequence of the primer.

2.2.1. Incorporation of a matched base

The binding of matched dGTP to the active site induces fingers together with stem IV loop rotating towards the active site (Fig. 1b), activating the chemical reaction of nucleotide incorporation. Since, in this conformation of the telomerase, the stem IV loop is not far away from stem III pseudoknot even after the rotation of fingers and stem IV toward the active site (or away from the stem III pseudoknot), the stem III pseudoknot is still in the folding conformation. Upon the completion of nucleotide incorporation, the binding site *A* binds to the new nearest unpaired base 47 on the template RNA, because the previous unpaired base 48 where the binding site *A* has just bound has disappeared due to base-pair formation. Note that the binding of site *A* to base 47 should overcome the elastic force and the affinity between the TEN and RT domains by the thermal noise. At the same time, the fingers together with stem IV loop rotate away from the nucleotide-free active site (Fig. 1c).

2.2.2. Incorporation of a mismatched base

Consider mismatched dTTP instead of dGTP in Fig. 1a binding to the active site. The fingers together with stem IV loop rotate towards the active site, activating the chemical reaction of nucleotide incorporation (Fig. 1a′). After the completion of nucleotide incorporation, the fingers together with stem IV loop rotate away from the nucleotide-free active site (Fig. 1b′). In this case, although the mismatched dTTP has been connected to the backbones of the nascent DNA primer, the mismatched base T is not paired with the sterically corresponding base C on the template RNA. Thus, the binding site *A* is still binding to the same unpaired base 48 and no movement of the active site relative to the RNA template occurs, the nucleotide addition becoming stalled [51], as in other polymerase enzymes such as replicative DNAP [52] and RNAP [53]. The stalling after the misincorporation gives sufficient time for the mismatched base on the 3′ end of primer to be cleaved [51]. After the mismatched base is excised, the matched dGTP binds, closing the fingers and stem IV loop (Fig. 1c′). As the matched dGTP is incorporated, the binding site *A* binds to the new nearest unpaired base 47 on the template RNA and, simultaneously, the fingers and stem IV loop rotate away from the nucleotide-free active site (Fig. 1c).

From Fig. 1c the next cycle of nucleotide incorporation proceeds similarly until the binding site *A* binds the last unpaired base 43 on the template (Fig. 1d), thus giving the processive nucleotide addition. Note that, as the active site is moved away from its equilibrium position—relative to the TEN and TRBD domains—near base 48, the stem IV loop becomes further and further away from the stem III pseudoknot, which may result in the unfolding of the stem III pseudoknot when the fingers and stem IV rotate towards the active site upon a nucleotide binding.

It is also interesting to note here that the movement of the RT domain containing the active site along the template may result in some residues upstream of the active site on the RT domain to unwind the DNA:RNA base pair at the 3′ end of the template, thus keeping the DNA:RNA hybrid with a limited number of base pairs. This is particularly important for telomerases with long template regions such as telomerase from *Euplotes aediculatus* [54] and that from yeast [55], circumventing the generation of very high base-pairing free energy required to disrupt during repeat addition translocation (see Section 2.3). For *T. thermophila* telomerase, where the template region is not long, even with all bases on the template region being paired with those of DNA primer, the DNA:RNA hybrid can be readily disrupted (see Section 3.3.1). Thus, for *T. thermophila* telomerase, the unwinding of the DNA:RNA base pair at the 3′ end of template may not be necessary. Nevertheless, we consider two cases in this work: with and without unwinding of the DNA:RNA base pair at the 3′ end of template.

2.3. Mechanism of processive repeat addition

In Fig. 1d, after the matched dGTP bind and is then incorporated, because the previously unpaired base 43 where the binding site *A* has just bound has disappeared due to base-pair formation, no unpaired base is left in the template region. Moreover, since the unpaired bases in the TBE region are bound to the TERT [18], no interaction exists now between telomerase RNA and the binding site *A*. On the other hand, because of the steric restriction of the primer, the motifs that consist of the binding site *A* and the active site are not allowed to move in the direction pointing towards the 5′ end of the primer (Fig. 1e). As a result, an elastic force, $F_p = -\mathrm{d}\, V_p(x)/\mathrm{d}\, x$, occurs, acting on the primer 3′ end by the motifs that contain the binding site *A* and the active site. Here, $V_p(x)$, the form of which will be given below (see Section 2.4), is the elastic potential resulting from the deviation of the RT domain from its equilibrium position relative to the TEN and TRBD domains, with x denoting the deviation. However, the elastic force F_p is not large enough to disrupt the DNA:RNA hybrid and the interaction of PAS with the primer.

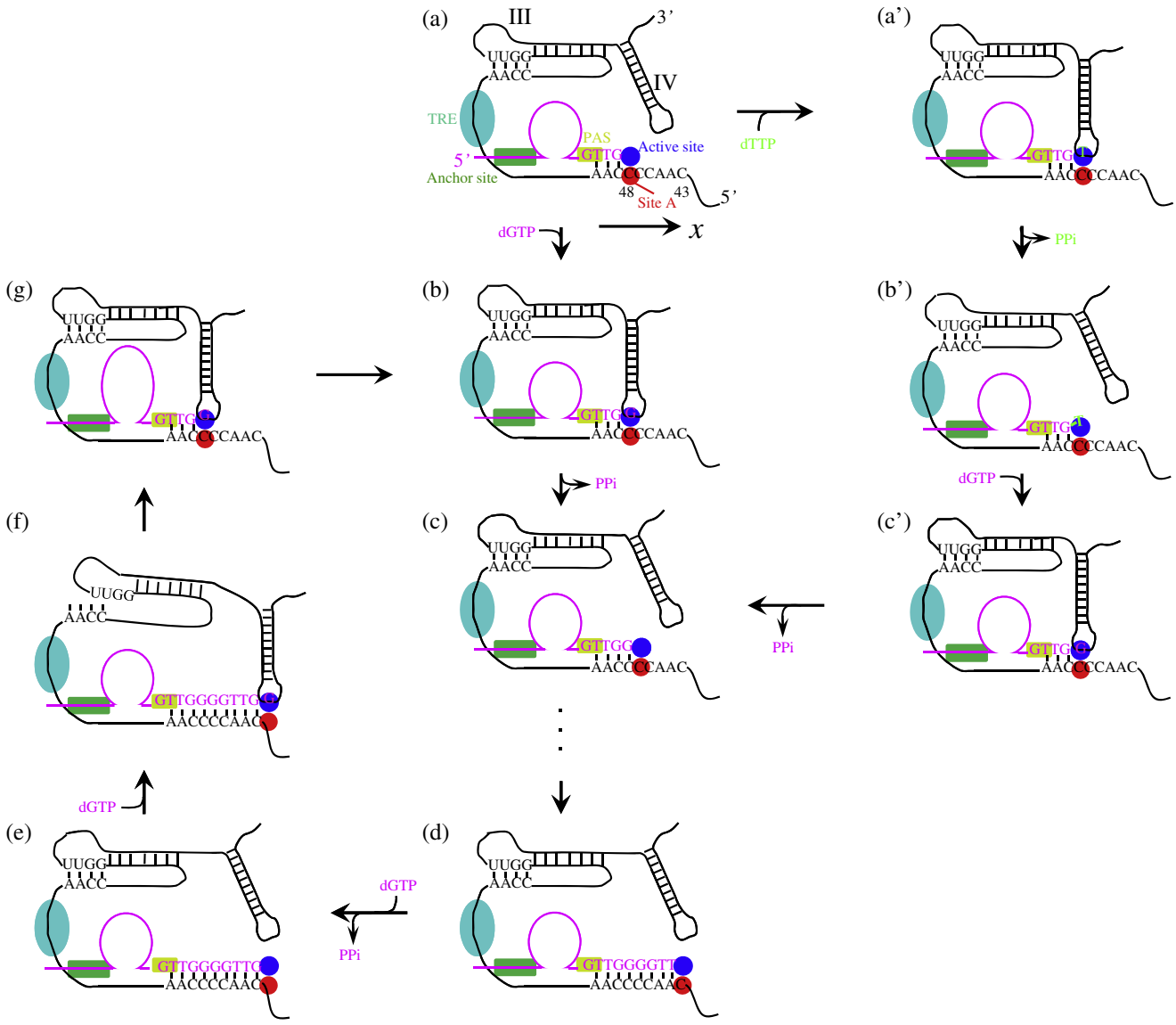

Fig. 1. Schematic illustrations of the proposed model for processive nucleotide and repeat additions by the recombinant *Tetrahymena* telomerase (see Section S5 in the Appendix for detailed legend). For clarity, the telomerase RNA is only drawn schematically and stems I and II are not shown. For TERT, only the template-binding site *A* (red dot), polymerase active site (blue dot), PAS, anchor site and binding site for TRE element are shown. The DNA primer is drawn in pink and, for clarity, the mismatched nucleotide or base is drawn in green.

Consider that the nucleotide dGTP binds to the active site in Fig. 1e,[1] inducing the fingers together with stem IV loop to rotate towards the active site. This in turn induces the stem IV loop becoming very far away from the stem III pseudoknot, thus resulting mechanically in the unfolding of the stem III pseudoknot (Fig. 1f). The unfolding of the stem III pseudoknot induces a force $F_{III} = -\mathrm{d}\, V_{III}(x)/\mathrm{d}\, x$, where $V_{III}(x)$, the form of which will be given below (see Section 2.4), is the interaction potential to make bases AACC and bases UUGG reform base pairs in the unfolding conformation of pseudoknot III or the potential to unfold the pseudoknot III. Now, both forces F_{III} and F_p are acting on the primer. This is different from the case before the incorporation of the nucleotide paired with the last base 43 on the template, where both F_p and F_{III} that occurs after the binding of dNTP to the active site are mainly acting on the template rather than the primer, because the binding site *A* is bound to the unpaired base 43 on the template.

In Fig. 1f, the total force of F_{III} and F_p may be large enough to disrupt the DNA:RNA hybrid and the interaction of PAS with the primer. Then the two forces F_p and F_{III} drive the RT domain that consists of the binding site *A* and the active site returned to the equilibrium position relative to the TEN and TRBD domains. Upon returning to the equilibrium position, the RT domain is stabilized in this position by its interaction with the TEN domain via residues such as Leu14 [50]. Then, the binding site *A* rebinds correctly the unpaired base 48, the PAS rebinds the DNA base opposite template base A51 and the next

[1] It has been experimentally shown that *Tetrahymena* telomerase has a K_m for dGTP incorporation that is about 10-fold lower than the K_m for incorporation of dTTP [62], which suggests that the active site has a much higher affinity for dGTP than dTTP. Since no unpaired base on the template is left in Fig. 1e, no conformational change of residues in the vicinity of the active site is induced by the strong binding of site *A* to an unpaired base. As a consequence, the active site has a much lower affinity for dNTP than that when the site *A* is bound strongly to an unpaired base such as in the case of Fig. 1d. Thus, in Fig. 1e the active site will be bound most probably by dGTP with a low binding rate. On the other hand, during the long period before dGTP binding under low dGTP concentration, no interaction exists between the template region of telomerase RNA and the TERT. As a result, the TERT has a large probability to dissociate from telomerase RNA in recombinant telomerases [20]. Therefore, the repeat addition processivity requires high dGTP concentrations or is stimulated allosterically by dGTP, independent of the template sequence (i.e., whether the first or last base on the template is C or A).

adjacent 5′ DNA base, and the primer 3′ end rebinds to the template via forming the TTG:AAC hybrid (Fig. 1g). Note here that, since the anchor site is bound to the 5′ end of the primer, during the very short period from the moment when the DNA:RNA hybrid and interaction of PAS with the primer are disrupted through the moment when the PAS rebinds to the primer and the TTG:AAC hybrid forms, the primer has a very small probability to detach from the telomerase. Note also that the presence of an affinity between the TEN and RT domains ensures the repeat addition processivity. Otherwise, if the affinity disappears by mutating residues such as Leu14 in the TEN domain, the RT domain will be, due to the thermal noise, readily fluctuated to deviate from the equilibrium position (where a zero elastic force is acting on the RT domain) rather than be stabilized there upon the RT domain returning to the equilibrium position (see Section S2 in the Appendix). It is thus expected that, after the disruption of the DNA:RNA hybrid and the interaction of PAS with the primer, the site *A* is most probable to bind the unpaired base other than the initial base 48 of the template. On the hand, the PAS in the TEN domain can still bind the DNA base opposite template base A51 and the next adjacent 5′ DNA base, with the formation of TTG:AAC hybrid. As a result, the active site is distanced away from the primer 3′ end and the primer cannot be extended. Thus, the repeat addition processivity is reduced significantly, consistent with the experimental data of Zaug et al. [50].

Fig. 1g is the same as Fig. 1b except that the active site is moved relative to the primer by a sequence repeat. From then on the next repeat will proceed, thus giving the repeat addition processivity.

In the above model for the repeat addition processivity, the force F_{III} plays an important role in the unpairing of DNA:RNA hybrid, which facilitates the repeat addition processivity. The force F_{III} results from the unfolding of the stem III pseudoknot (or results from the potential to make bases AACC and bases UUGG reform base pairs in the unfolding conformation of pseudoknot III) when stem IV is rotated towards the nucleotide-bound active site in the position as shown in Fig. 1f. This implies that both the stem III pseudoknot and the stem IV are important to generate repeat addition processivity, which is in agreement with the previous experimental results [20]. Moreover, the unfolding of stem III pseudoknot that can be mechanically induced by the rotation of the stem IV loop away from it implies that the stem III pseudoknot is not bound to TERT, which is consistent with the fact that, up to now, no experimental result has shown that the stem III pseudoknot is bound to TERT.

2.4. Equation to describe the movement of active site

Based on the present model, the motion of the RT domain containing the binding site *A* and active site relative to the TEN and TRBD domains can be described by the following Langevin equation

$$\Gamma\frac{dx}{dt} = -\frac{\partial(V_A + V_H + V_{PAS} - V_P - V_{III})}{\partial x} + \xi(t), \quad (1)$$

where x denotes the position of the binding site *A* along template RNA and the viscous load acting on the RT domain is contained in the drag coefficient Γ. The potentials V_A, V_H, V_{PAS}, V_P and V_{III} will be discussed below. The last term, $\xi(t)$, denotes the thermal noise, with $\langle\xi(t)\rangle = 0$ and $\langle\xi(t)\xi(t')\rangle = 2k_BT\Gamma\delta(t-t')$. In Eq. (1), for simplicity, the interaction potential between the TEN and RT domains is not included, because it has no effect on the motion of the RT domain when it is not very close to the TEN domain. Note that the difference between Eq. (1) of the present work and that of the previous work [34] is the addition of potential V_{PAS} here. In other words, the total potential $(V_A + V_H - V_P - V_{III})$ in the first term on the right-hand side of Eq. (1) in the previous work [34] is replaced by $(V_A + V_H + V_{PAS} - V_P - V_{III})$ in the present work.

V_A represents the interaction potential between the binding site *A* and unpaired bases on the template. Before the incorporation of the nucleotide paired with base 48 on the template, V_A is shown in Fig. 2a,

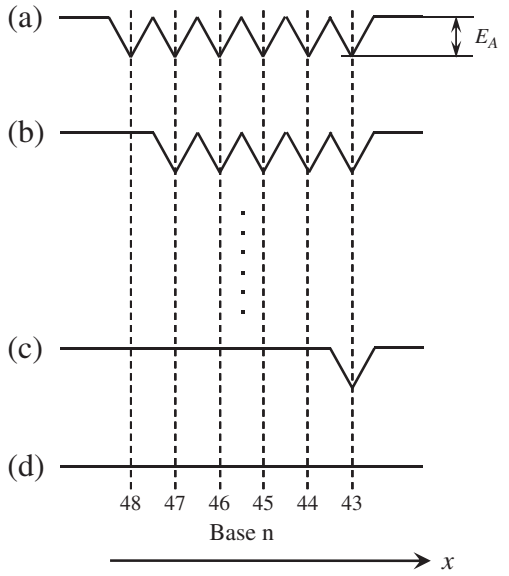

Fig. 2. Interaction potential, V_A, between template-binding site *A* and unpaired bases on the template. Before the incorporation of the nucleotide paired with base 48 on the template, V_A is shown in a. After the incorporation of the nucleotide paired with base 48 and before the incorporation of the nucleotide paired with base 47, V_A is shown in b. Then with the processive nucleotide incorporation V_A is changed similarly. After the incorporation of the nucleotide paired with base 44 and before the incorporation of the nucleotide paired with base 43, V_A becomes the one as shown in c. After the incorporation of the nucleotide paired with the last base 43, V_A becomes the one as shown in d.

with the potential depth, E_A, the binding affinity.[2] After the incorporation, V_A is changed to that as shown in Fig. 2b, because the unpaired base 48 has disappeared due to base-pair formation and thus no interaction exists between the binding site *A* and base 48 on the template. Then, with the processive nucleotide incorporation, V_A is changed similarly. After the incorporation of the nucleotide paired with base 44, V_A becomes the one as shown in Fig. 2c. Then, after the incorporation of dGTP paired with the last base 43, V_A becomes the one as shown in Fig. 2d, implying that no interaction exists between the binding site *A* and the template because all the bases on the template are paired with the primer to form the DNA:RNA duplex.

V_H represents the potential of the motifs that contain the binding site *A* and the active site interacting with the DNA:RNA hybrid, which is related to the free-energy change required to disrupt the DNA:RNA hybrid. Consequently, the depth, E_H, of the potential V_H is approximately equal to the free-energy change to disrupt the hybrid. By using parameters for the nearest-neighboring thermodynamic model for RNA:DNA duplex stabilities [56], we have the following results: $E_H = 0.9$ kcal/mol (~1.5 k_BT) for 5′-CCAA-3′:3′-GGTT-5′, $E_H = 3$ kcal/mol (~5.1 k_BT) for 5′-CCCAA-3′:3′-GGGTT-5′, $E_H = 5.1$ kcal/mol (~8.6 k_BT) for 5′-CCCCAA-3′:3′-GGGGTT-5′, $E_H = 7.2$ kcal/mol (~12 k_BT) for 5′-ACCCCAA-3′:3′-TGGGGTT-5′, $E_H = 8.2$ kcal/mol (~14 k_BT) for 5′-AACCC-CAA-3′:3′-TTGGGGTT-5′, $E_H = 9.1$ kcal/mol (~15 k_BT) for 5′-CAACCC-CAA-3′:3′-GTTGGGGTT-5′.[3] From these values of E_H, the approximate forms of potential V_H are shown in Fig. 3. In above calculations, we have considered the case that no unwinding of the DNA:RNA base pair at the 3′

[2] As it is known, the dynamics for a Brownian particle to escape from one potential well depends mainly on the well depth of the potential while is insensitive to the form of the potential (see. e.g., Ref. [66]). Thus, the calculated results presented in this work depend mainly on values of the well depth of the potential while forms of the potential are not important.

[3] In the previous work [34], E_H was calculated by taking the value of each dimer duplex (rNN:dNN) having the orientation of 3′-rNN-5′:5′-dNN-3′, where rNN represent two RNA bases and dNN represent two DNA bases forming base pairs with the two rNN. Here, the orientation of the dimer duplex is taken as 5′-rNN-3′:3′-dNN-5′, which is consistent with that taken in Ref. [56]. This gives values of E_H determined here different from those determined in the previous work.

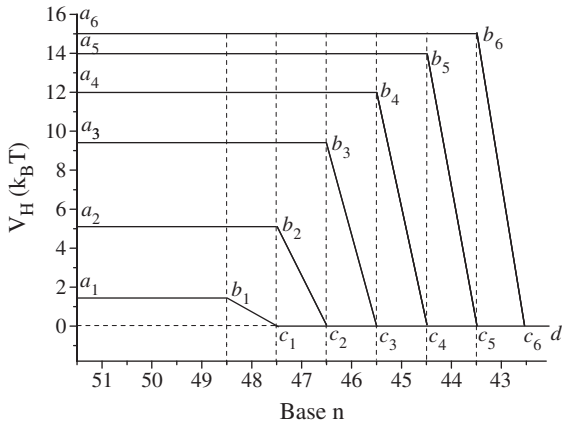

Fig. 3. Interaction potential, V_H, of the motifs that consist of the binding site *A* and the active site with the DNA:RNA hybrid. After the incorporation of the nucleotide paired with base 48 and before the incorporation of the nucleotide paired with base 47, V_H is represented by curve $a_1b_1c_1d$. After the incorporation of the nucleotide paired with base 47 and before the incorporation of the nucleotide paired with base 46, V_H is represented by curve $a_2b_2c_2d$. After the incorporation of the nucleotide paired with base 46 and before the incorporation of the nucleotide paired with base 45, V_H is represented by curve $a_3b_3c_3d$. After the incorporation of the nucleotide paired with base 45 and before the incorporation of the nucleotide paired with base 44, V_H is represented by curve $a_4b_4c_4d$. After the incorporation of the nucleotide paired with base 44 and before the incorporation of the nucleotide paired with base 43, V_H is represented by curve $a_5b_5c_5d$. After the incorporation of the nucleotide paired with the last base 43, V_H is represented by curve $a_6b_6c_6d$.

end of template occurs. The results for the dynamics of repeat addition processivity based on these values of E_H are given in the main text. For the case that the unwinding of the DNA:RNA base pair at the 3′ end of template occurs (see last paragraph in Section 2.2), the calculated results of E_H and the corresponding results for the dynamics of repeat addition processivity are presented in the Appendix (see Section S4).

V_{PAS} represents the interaction potential of PAS with the DNA base T opposite template base A51 and the next adjacent 5′ DNA base G. Similar to Fig. 2, the form of V_{PAS} is shown in Fig. 4, with the binding affinity E_{PAS}, the value of which will be discussed below (see Section 3.1).

V_P represents the elastic potential resulting from the deviation of the RT domain from the equilibrium position relative to the TEN and TRBD domains. It can be written as $V_P = -\frac{1}{2}C_p x^2$, where C_p is the elastic coefficient and $x = 0$ is located in the position of base 48. Since the elastic coefficient C_p is not available for the connection residues, we can estimate its value with the experimental data for other proteins. Using neutron spin-echo spectroscopy, Bu et al. [57] obtained the elastic coefficient of about 8.5 pN/nm for the connection residues between the polymerase and 5′-nuclease domains of DNA polymerase from *Thermus aquaticus*. Zaccai [58] determined an elastic coefficient of about 30 pN/nm for the myoglobin. Thus, we infer that the elastic coefficient of the connection residues between the domain (the TEN and TRBD domain) containing the anchor site and the RT domain containing the binding site *A* and the active site in TERT is in the range of about 8.5–30 pN/nm.[4]

V_{III} represents the interaction potential to make bases AACC and bases UUGG reform base pairs in the unfolding conformation of pseudoknot III when a nucleotide is bound to the active site. When bases AACC are close to bases UUGG, the interaction energy is approximately equal to the free-energy change required to unfold the stem III pseudoknot. Since, in the folding conformation of the stem III pseudoknot, the stem IV loop is assumed to position around base 48 of

[4] In the previous work [34], for simplicity of analysis, the elastic coefficient was taken to be $C_p = 0$.

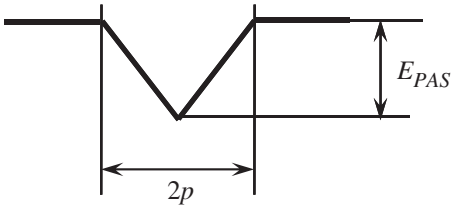

Fig. 4. Interaction potential of PAS with the DNA base T opposite template base A51 and the next adjacent 5′ DNA base.

the template, it is considered that when the binding site *A* binds to base 48 or the nearby bases such as base 47 and base 46 the pseudoknot III is not required to unfold when stem IV rotates towards the active site. This implies that the potential depth of V_{III}, i.e., the free-energy change required to unfold pseudoknot III, $E_{III} \approx 0$. However, as the binding site *A* (or the active site) becomes further and further away from base 46, the stem III pseudoknot becomes partially unfolded or completely unfolded when stem IV rotates towards the active site upon a nucleotide binding. Thus, E_{III} increases gradually from 0 to the maximum value that corresponds to the completely unfolding conformation of the stem III pseudoknot. By using parameters for the nearest-neighboring thermodynamic model for RNA:RNA duplex stabilities [59], we obtain that the free-energy change to unfold pseudoknot 5′-AACC-3′:3′-UUGG-5′ is 2.5 kcal/mol (~4.2 k_BT), i.e., in the completely unfolding conformation $E_{III} = 2.5$ kcal/mol (~4.2 k_BT). For simplicity, we take E_{III} increasing linearly with the increase of the distance between the binding site *A* or the active site and base 46, i.e., $E_{III} = 1.1\ k_BT$ when the site *A* is positioned at base 45, $E_{III} = 2.1\ k_BT$ when the site *A* is positioned at base 44, $E_{III} = 3.2\ k_BT$ when the site *A* is positioned at base 43, $E_{III} = 4.2\ k_BT$ when the site *A* is positioned slightly beyond base 43. Thus, when the site *A* is positioned at base *n* ($n = 45, 44, 43$) or positioned slightly beyond base 43, the potentials V_{III} approximately have the similar forms to V_H shown in Fig. 3 but with the potential depths E_{III} as determined just above. When the active site is nucleotide-free, E_{III} is always nearly equal to 0 because the stem III pseudoknot is in the folding conformation.

It is noted that, since the telomeric repeats are G-rich, they could form G–G hairpin and G-quadruplex structures, which could influence the disruption of the DNA:RNA hybrid. Here, for simplicity of analysis, in Eq. (1) we do not consider the effect of the possible formation of the G–G hairpin and G-quadruplex structures on the RT translocation during repositioning of the active site after each round of repeat synthesis.

3. Results and discussion

3.1. Determination of the binding affinity of PAS to DNA primer

Experimental data of Baran et al. [46] indicated that the minimal lengths required for primers to be extended by the *Tetrahymena* telomerase depend on the positions along the template at which the primers are initially aligned as well as the primer concentration. At a moderate primer concentration of 2.5 μM, the minimal lengths are 4, 5, and 6 nt when the primers are aligned in the beginning (Fig. 5a), middle (Fig. 5b) and next to the end (Fig. 5c) to template, respectively. These data imply that, for the three cases, the binding affinities of the primers to the telomerase are just larger than or nearly equal to a critical affinity, E_c, under which the association time of the primer of a given concentration with the telomerase is approximately equal to the time for the telomerase to extend a DNA base. Now, we determine the binding affinity E_{PAS} of the PAS to DNA primer using these experimental data.

Based on our present model, it is seen that, when the primer is aligned in the next to the end to the template (Fig. 5c), the binding of the telomerase to the DNA primer is only via the formation of the DNA:RNA hybrid; when the primer is aligned in the beginning of the template (Fig. 5a), the binding of the telomerase to the DNA primer is via both the

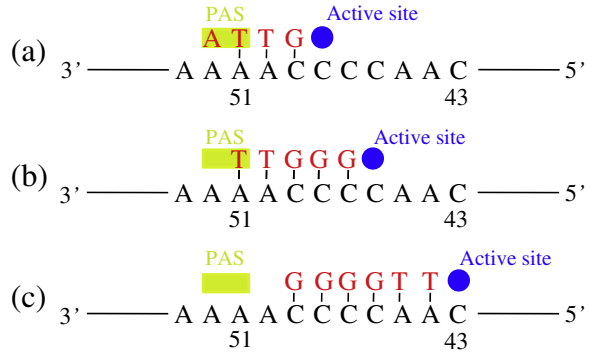

Fig. 5. A scheme illustrating the minimal lengths required for primer aligned in the beginning (a), middle (b) and next to the end (c) of the template to be extended with the *Tetrahymena* telomerase. The DNA sequences in a, b and c designate the shorted primers measured by Baran et al. [46] at a moderate primer concentration of 2.5 μM.

formation of the DNA:RNA hybrid and the interaction of PAS with two DNA bases A and T; when the primer is aligned in the middle of the template (Fig. 5b), the binding of the telomerase to the DNA primer is via both the formation of the DNA:RNA hybrid and the interaction of PAS with one DNA bases T. For the case of Fig. 5c, the binding affinity, E_3, of the telomerase to the DNA primer can be calculated by using parameters for the nearest-neighboring thermodynamic model for RNA:DNA duplex stabilities [56], which is obtained to be $E_3 = 6.3$ kcal/mol (~11 k_BT) for 5′-AACCCC-3′:3′-TTGGGG-5′. As mentioned above, we have $E_c \approx E_3 = 6.3$ kcal/mol (~11 k_BT). For the case of Fig. 5a, by using parameters for the nearest-neighboring thermodynamic model it is obtained that base-pairing of 5′-CAA-3′:3′-GTT-5′ nearly has no contribution for the stability of the telomerase and the primer. Thus, the binding affinity of the telomerase to the primer is only determined by that of PAS to the primer. As a result, we have $E_1 = E_{PAS} \approx E_c = 6.3$ kcal/mol. For the case of Fig. 5b, by using parameters for the nearest-neighboring thermodynamic model it is obtained that the free-energy change to disrupt 5′-CCCAA-3′:3′-GGGTT-5′ hybrid is 3 kcal/mol. Considering that the homologous binding affinity of the PAS to DNA bases, we have the binding affinity of the telomerase to the DNA primer for the case of Fig. 5b, $E_2 = E_{PAS}/2 + 3$ kcal/mol = 6.15 kcal/mol, which is nearly equal to the value of critical affinity E_c.

Instead of the primers shown in Fig. 5, consider a primer 3′-GTT-5′ in Fig. 5a, a primer 3′-GGGT-5′ in Fig. 5b and a primer 3′-TTGGG-5′ in Fig. 5c. Using parameters for the nearest-neighboring thermodynamic model and $E_{PAS} = 6.3$ kcal/mol, we have $E_1' = E_{PAS}/2 = 3.15$ kcal/mol, $E_2' = 2$ kcal/mol and $E_3' = 4.2$ kcal/mol. These values of E_1', E_2' and E_3' are evidently smaller than the critical affinity E_c. Thus these primers of concentration of 2.5 μM cannot be extended by the telomerase.

3.2. Dissociation probability of primer from telomerase

3.2.1. Dissociation probability during period of transition from previous round of repeat addition to next one

In this section, we study the dissociation probability of the primer from telomerase during the time period of the transition from the previous round of repeat addition to the next one. In the present model, this corresponds to the time period from the moment when dGTP paired with the last base C43 on the template is incorporated through the moment when the binding site *A* rebinds to the unpaired base C48 of template, the PAS rebinds to the primer, and the TTG:AAC hybrid forms. The period can be considered to be composed of two periods: one period (called period P_2) from the moment of the completion of the incorporation of dGTP paired with the last base C43 on the template through the moment when one repeat of DNA:RNA hybrid and the interaction of PAS with the primer are disrupted; the other period (called period P_1) from the moment when the repeat of DNA:RNA hybrid and the interaction of PAS with the primer are disrupted through the moment when the binding site *A* rebinds to the unpaired base C48, the PAS rebinds to the primer and the TTG:AAC hybrid forms.

First, we study the dissociation probability during period P_1. As mentioned before, upon the RT domain returning to the equilibrium position relative to the TEN domain, the TERT is stabilized in this equilibrium conformation by the interaction of the TEN domain with the RT domain via residues such as Leu14 in the TEN domain [50]. This ensures the rapid rebinding of site *A* to the initial unpaired base 48, the rebinding of PAS to the DNA base opposite template base A51 and the next adjacent 5′ DNA base, and the formation of TTG:AAC hybrid. Thus, the time of period P_1 should be calculated by $T_m + T_b$. Here T_m denotes the mean time for the RT domain to move to the equilibrium position after the DNA:RNA hybrid and the interaction of PAS with the primer are disrupted; while T_b denotes the mean time for the site *A* to rebind the unpaired base 48, the PAS to rebind the DNA base opposite template base A51 and the next adjacent 5′ DNA base and the TTG:AAC hybrid to form after the RT domain returns to the equilibrium position.

Now, we determine T_m. As seen in Eq. (1), during the period P_1, the movement of the RT domain relative to the TEN and TRBD domains is described by the following Langevin equation

$$\Gamma \frac{dx}{dt} = -C_p x + \xi(t). \tag{2}$$

where the RT domain is initially positioned at $x = 6p$ ($p = 0.34$ nm) and is finally positioned at $x = 0$. Using the similar derivation procedure as used in Xie [34], from Eq. (2) the mean first-passage time for the RT domain to move from $x = 6p$ to $x = 0$ can be calculated by the following equation

$$T_m = \frac{\Gamma}{k_B T} \int_0^{6p} \exp\left[\frac{1}{2k_B T} C_p (y-6p)^2\right] dy \int_0^{y} \exp\left[-\frac{1}{2k_B T} C_p (z-6p)^2\right] dz. \tag{3}$$

Using Eq. (3), the calculated results of T_m versus C_p are shown in Fig. 6a for $\Gamma = 5.65 \times 10^{-11}$ kg s^{-1} that is obtained from the Stokes drag coefficient $\Gamma = 6\pi\eta r$ on the RT domain with the diameter of $2r = 6$ nm [25], where the viscosity $\eta = 0.01$ gcm^{-1} s^{-1}. As expected, T_m decreases with the increase of C_p. It is seen that T_m is very short, with the time in the range from about 0.01 μs for $C_p = 8.5$ pN/nm to about 0.004 μs for $C_p = 30$ pN/nm.

To obtain the dissociation time of the primer from the telomerase, we consider the movement of the primer relative to the telomerase, which is described by the following Langevin equation

$$\Gamma_{\mathrm{DNA}} \frac{dy}{dt} = -\frac{dU(y)}{dy} + \zeta(t), \tag{4}$$

where y denotes the position of the primer relative to the telomerase and Γ_{DNA} is the frictional drag coefficient on the primer. $\zeta(t)$ is the thermal noise, with $\langle \zeta(t) \rangle = 0$ and $\langle \zeta(t)\zeta(t') \rangle = 2k_B T \Gamma_{\mathrm{DNA}} \delta(t-t')$. The interaction potential of the primer with the telomerase can be written in the following Morse form $U(x) = U_0[\exp(-2y/B) - 2\exp(-y/B)]$, where U_0 is the binding affinity and B is the interaction distance that is taken to be 1 nm (the Debye length in solution). Similar to the derivation of Eq. (3) from Eq. (2), from Eq. (4) we have the following equation for the mean first-passage time, T_d, for the primer to move a distance of L from the telomerase

$$T_d = \frac{\Gamma_{\mathrm{DNA}}}{k_B T} \int_0^{L} dy \cdot \exp\left\{U_0\left[\exp\left(-\frac{2y}{B}\right) - 2\exp\left(-\frac{y}{B}\right)\right] / k_B T\right\} \cdot \int_0^{y} dz \cdot \exp\left\{-U_0\left[\exp\left(-\frac{2z}{B}\right) - 2\exp\left(-\frac{z}{B}\right)\right] / k_B T\right\}. \tag{5}$$

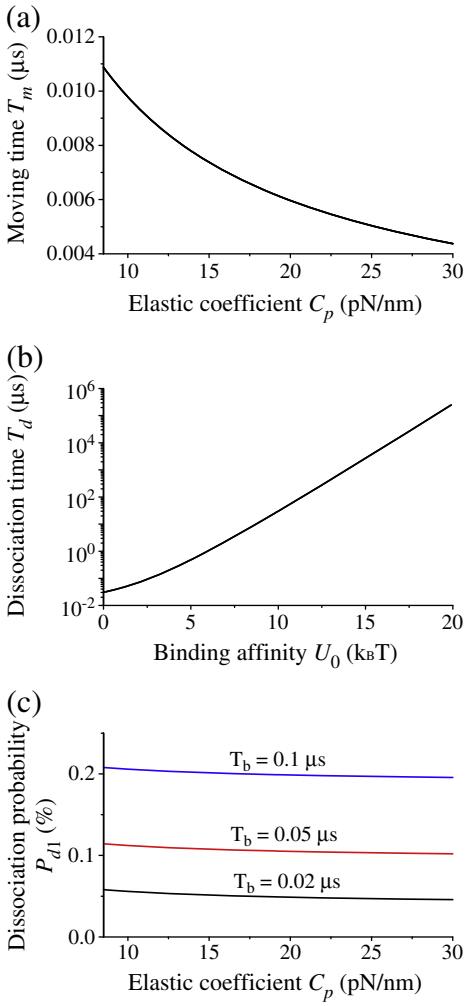

Fig. 6. Results for the dissociation of primer from telomerase during the period from the moment when one repeat of DNA:RNA hybrid and the interaction of PAS with the primer are disrupted to the moment when the site *A* binds the unpaired base 48 of the template, the PAS rebinds to the primer and the TTG:AAC hybrid forms. (a) The mean time, T_m, for the RT domain to move to the equilibrium position after the disruption of the DNA:RNA hybrid and the interaction of PAS with the primer versus the elastic coefficient C_p. (b) The mean time, T_d, for the primer to detach from the telomerase versus the binding affinity U_0 between them. (c) The dissociation probability P_{DNA1} versus elastic coefficient C_p for different values of T_b, the mean time for the site *A* to bind the unpaired base 48 after the RT domain returns to the equilibrium position.

It is considered that the primer detaches from the telomerase when its moves away from the telomerase by a distance of $L = 5$ nm that is larger than $B = 1$ nm. In the calculation, we take $\Gamma_{DNA} = 1 \times 10^{-11}$ kg s^{-1}, which is equivalent to the drag coefficient on a sphere of radius of about 0.5 nm. Using Eq. (5), the calculated results of the mean time T_d for the primer to detach from the telomerase versus the binding affinity U_0 are shown in Fig. 6b. As expected, T_d increases significantly with the increase of U_0.

The dissociation probability of the primer from the telomerase during period P_1 is obtained as follows

$$P_{DNA1} = \frac{T_m + T_b}{T_m + T_b + T_d}. \quad (6)$$

From the experimental evidence [46–48], it appears that the PAS is composed of two residues Trp187 and Phe178 in *Tetrahymena* TEN domain that interact with the primer, while the anchor site is composed of one residue Gln168 in TEN domain and residues in other domains [46–49]. Thus, it is expected that the binding affinity of the anchor site to the primer should be at least larger than the binding affinity of the PAS to the primer, i.e., $U_0 \geq E_{PAS} = 6.3$ kcal/mol (~11 k_BT). Taking different values of $T_b > T_m$, using Eq. (6) and the results given in Fig. 6a and b, we show the results of the dissociation probability P_{DNA1} versus elastic coefficient C_p in Fig. 6c for $U_0 = 11$ k_BT. It is seen that, even for the conservative values of $U_0 = 11$ k_BT and $C_p = 8.5$ pN/nm, the primer has a negligible probability to detach from the telomerase during period P_1.

Here, it is interesting to note that the experimental results that the minimal lengths required for primers to be extended with the telomerase by multiple repeats are the same as those by a single nucleotide [46] can be understood by using the results of Fig. 6a and b and Eq. (6). In the experiment [46], during the period of the transition from the first round of repeat addition to the second one, no interaction exists between the anchor site and the primer. In our model, this is equivalent to $U_0 = 0$. From Fig. 6b, we see that the mean dissociation time $T_d = 0.03$ μs at $U_0 = 0$. From Fig. 6a, we seen that, in the range of $C_p = 8.5$–30 pN/nm, $T_m = 0.01$–0.004 μs. Thus, using Eq. (6) we have the dissociation probability $P_{d1} = 50\%$–44% for $T_b = 0.02$ μs. This implies that, during the period of the transition from the first round of repeat addition to the second one, more than 50% of the primers cannot be dissociated from the telomerase for $T_b = 0.02$ μs. Thus, the minimal lengths required for primers to be extended with the telomerase by multiple repeats can be approximately said to be the same as those by a single nucleotide.

Then, we study the dissociation probability during period P_2 from the moment of the completion of the incorporation of dGTP paired with the last base C43 on the template through the moment when one repeat of DNA:RNA hybrid and the interaction of PAS with the primer are disrupted.

During this period P_2, as shown in Fig. 1f, the interaction between the primer and telomerase consists of three affinities between them, i.e., the affinity of anchor site for the primer, the affinity of PAS for the primer and the affinity of template for the primer via forming base-pairing. As determined in Section 2.4, the last affinity is $E_H = 9.1$ kcal/mol. As determined in Section 3.1, the affinity of PAS for the primer is $E_{PAS} = 6.3$ kcal/mol. As discussed just above, the affinity of the anchor site for the primer is $U_0 \geq E_{PAS} = 6.3$ kcal/mol. Thus the total affinity is $E_T = E_H + E_{PAS} + U_0 \geq 21.7$ kcal/mol (~36.7 k_BT). From Eq. (5), we obtain that, for this value of E_T, the mean dissociation time is at least 1.9×10^6 s, which is much larger than the lifetime of period P_2 (see Section 3.3.1). Thus, the dissociation probability of the primer from the telomerase during period P_2 can be negligible.

Taken together, we conclude that, during the period of the transition from previous round of repeat addition to the next one, the dissociation probability of the primer from the telomerase is negligibly small.

3.2.2. Dissociation probability during period of nucleotide addition

At the initiation of each nucleotide addition period (see, e.g., Fig. 1a and b), the interaction between the primer and telomerase consists of only two affinities, i.e., the affinity of the anchor site and that of the PAS for the primer, because, based on the parameters for the nearest-neighboring thermodynamic model [56], the base-pairing of 5′-CAA-3′:3′-GTT-5′ nearly has no contribution for the stability of the primer–telomerase complex. Thus the total affinity of the primer for the telomerase is $E_T = E_{PAS} + U_0 \geq 12.6$ kcal/mol (~21.3 k_BT). From Eq. (5), we obtain that, for this value of E_T, the mean dissociation time is equal to or larger than 0.91 s, which is in the same order of the mean time for incorporation of a nucleotide.

During the incorporation of the second nucleotide, the affinity of template for the primer via forming base-pairing is $E_H = 0.9$ kcal/mol. Thus, the total affinity of the primer with the telomerase is $E_T = E_H + E_{PAS} + U_0 \geq 13.5$ kcal/mol (~22.8 k_BT). From Eq. (5), we obtain that, for this value of E_T, the mean dissociation time is equal to or larger than 3.8 s, which is in the same order of the mean time for incorporation of a nucleotide.

Table 1
Conservative values of mean dissociation time and dissociation probability of primer from telomerase during period of nucleotide additions.

Order of nucleotides	1st	2nd	3rd	4th	5th	6th
Dissociation time (s)	0.91	3.8	110	3.1×10^{3}	8.9×10^{4}	4.5×10^{5}
Dissociation probability	0.52	0.21	9×10^{-3}	3.3×10^{-4}	1.1×10^{-5}	2.2×10^{-6}

Similarly, we can obtain the least values of the mean dissociation time during the incorporations of other nucleotides. The results are summarized in Table 1. Using these least values and taking the mean time for incorporation of a nucleotide as 1 s, the calculated results for the largest values of the dissociation probability during incorporation of different nucleotides are shown in Table 1. From the results shown in Table 1 and the results presented in Section 3.2.1, it is seen that, during the processive nucleotide and repeat additions, the dissociation of the primer from the telomerase occurs mainly during the incorporation of the 1st nucleotide.

It is noted here that the calculated results show that the dissociation of the primer from the telomerase is dependent on the number of base pairs. However, the experimental data indicated that the dissociation of the primer from the telomerase is nearly independent on the amount of base-pairing between primer and template for a given length of primer (e.g., 18 nt) [49,60]. The difference between our calculated results and the experimental data may be due to the following reason. It should be noted that, for the fixed length of primer, if the number of bases on primer paired with the template is reduced, the interaction length of the primer with TERT should be increased accordingly. Thus, the decrease of the affinity due to the base paring may be partially compensated by the increase of the affinity between TERT and the primer. This is consistent with the experimental data showing that the dissociation enhances with the reduction of the primer length [49]. Moreover, since no base on primer is paired with the template in the absence of RNA, the interaction length of the primer with TERT should be larger than that in the presence of RNA. On the other hand, no base-pairing is present in the absence of RNA while the base-pairing exists in the presence of RNA. The two effects may induce the binding affinity of the primer for the telomerase in the absence of RNA slightly smaller than that in the presence of RNA, resulting in that the dissociation of the primer from the telomerase in the absence of RNA only slightly larger than in the presence of RNA. By contrast, in our calculation we considered a complete interaction between TERT and the primer for different numbers of base pairs.

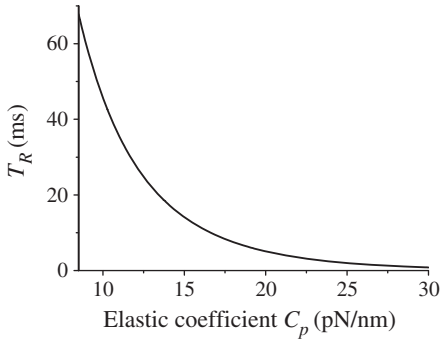

Fig. 7. Results for the effect of the elastic coefficient C_p on the mean time T_R taken to disrupt the DNA:RNA hybrid and then reposition the primer 3′ end to the beginning of the template after the incorporation of dGTP paired with the last base C43 on the template.

3.3. Dynamics of repeat addition processivity

In the previous work [34], we have studied the dynamics of processive repeat addition, which has not considered (i) the effect of the interaction of PAS with the primer, (ii) the effect of primer dissociation and (iii) the effect of the elastic force resulting from the non-zero elastic coefficient C_p. In this section, we re-study the dynamics with the addition of the three effects.

We denote T_R the time taken to disrupt the DNA:RNA hybrid and then reposition the primer 3′ end to the beginning of the template after the incorporation of the nucleotide paired with base n ($n=47$, 46, 45, 44, 43) on the template. Similar to derivation in the previous work, from Eq. (1) we obtain the mean time T_R approximately having the following form

$$\begin{aligned}
T_R = {} & \frac{\Gamma}{k_BT}\int_0^{p/2} dy \exp\left[\frac{2E_A+E_H+E_{PAS}-E_{III}}{pk_BT}y+\frac{C_p(y-X)^2}{2k_BT}\right] \\
& \times\int_0^{p/2}\exp\left[-\frac{2E_A+E_H+E_{PAS}-E_{III}}{pk_BT}z-\frac{C_p(z-X)^2}{2k_BT}\right]dz \\
& +\frac{\Gamma}{k_BT}\int_{p/2}^{p} dy \exp\left[\frac{E_A}{k_BT}+\frac{E_H+E_{PAS}-E_{III}}{pk_BT}y+\frac{C_p(y-X)^2}{2k_BT}\right] \\
& \times\int_0^{p/2}\exp\left[-\frac{2E_A+E_H+E_{PAS}-E_{III}}{pk_BT}z-\frac{C_p(z-X)^2}{2k_BT}\right]dz \\
& +\frac{\Gamma}{k_BT}\int_{p/2}^{p} dy \exp\left[\frac{E_H+E_{PAS}-E_{III}}{pk_BT}y+\frac{C_p(y-X)^2}{2k_BT}\right] \\
& \times\int_{p/2}^{p}\exp\left[-\frac{E_H+E_{PAS}-E_{III}}{pk_BT}z-\frac{C_p(z-X)^2}{2k_BT}\right]dz \\
& +\frac{\Gamma}{k_BT}\int_{p}^{X} dy \exp\left[\frac{E_A+E_H+E_{PAS}-E_{III}}{k_BT}+\frac{C_p(y-X)^2}{2k_BT}\right] \\
& \times\int_0^{p/2}\exp\left[-\frac{2E_A+E_H+E_{PAS}-E_{III}}{pk_BT}z-\frac{C_p(z-X)^2}{2k_BT}\right]dz \\
& +\frac{\Gamma}{k_BT}\int_{p}^{X} dy \exp\left[\frac{E_H+E_{PAS}-E_{III}}{k_BT}+\frac{C_p(y-X)^2}{2k_BT}\right] \\
& \times\int_{p/2}^{p}\exp\left[-\frac{E_H+E_{PAS}-E_{III}}{pk_BT}z-\frac{C_p(z-X)^2}{2k_BT}\right]dz \\
& +\frac{\Gamma}{k_BT}\int_{p}^{X} dy \exp\left[\frac{C_p(y-X)^2}{2k_BT}\right]\int_{p}^{y}\exp\left[-\frac{C_p(z-X)^2}{2k_BT}\right]dz,
\end{aligned} \tag{7}$$

where $X=6p$ after the incorporation of the nucleotide paired with the last base 43, $X=5p$ after the incorporation of the nucleotide paired with base 44, $X=4p$ after the incorporation of the nucleotide paired with base 45, etc. Note that, after dGTP paired with the last base C43 on the template is incorporated, $E_A=0$ in Eq. (7).

3.3.1. Wild-type telomerase RNA

After the incorporation of dGTP paired with the last base 43, $E_A=0$, V_H becomes one that is represented by curve $a_6b_6c_6d$ in Fig. 3, with $E_H=15\ k_BT$, and the free-energy change required to unfold pseudoknot III is $E_{III}=4.2\ k_BT$. With $E_{PAS}=11\ k_BT$, $X=6p$ and $\Gamma=5.65\times10^{-11}$ kg s^{-1} determined before, from Eq. (7) the calculated results of T_R versus elastic coefficient C_p are shown in Fig. 7. It is seen that, in the range of $C_p=8.5$–30 pN/nm, $T_R\approx68$–0.83 ms. These values of T_d are so short that it ensures the RT domain having a small probability to deviate from the DNA:RNA hybrid by a sufficient distance along the direction perpendicular to the central axis (i.e., the x axis shown in Fig. 1a) of the hybrid so that the RT domain would return to the equilibrium position relative to the TEN and TRBD domains without disruption of the hybrid. If this occurs, the nucleotide addition activity would terminate. Note that, in the absence of the interaction of the

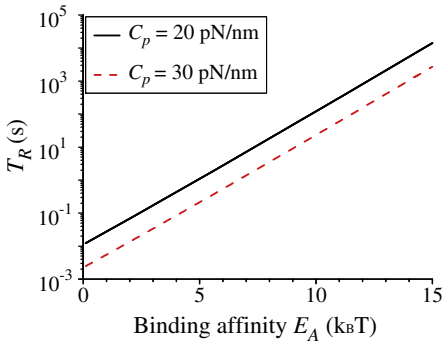

Fig. 8. Results for the effect of binding affinity E_A of binding site A on the time T_R taken to disrupt the DNA:RNA hybrid and then reposition the primer 3′ end to the beginning of the template after the incorporation of dTTP paired with the with base A44 on the template.

RT with the template, the RT domain is easily deviated from the template. The small deviation probability gives high repeat addition processivity.

Next, we calculate the time taken to disrupt the DNA:RNA hybrid and then reposition the product 3′ end before the incorporation of dGTP paired with the last base C43. For this case, $E_A \neq 0$. As an example, we consider the case that dTTP paired with base A44 has been incorporated. For this case, V_H becomes one represented by curve $a_5b_5c_5d$ in Fig. 3, with $E_H = 14\ k_BT$, and the free-energy change required to unfold pseudoknot III is $E_{III} = 3.2\ k_BT$ (see Section 2.4). Using Eq. (7) and with $E_{PAS} = 11\ k_BT$ and $X = 5p$, the calculated results of T_R versus E_A for two values of C_p are shown in Fig. 8. It is seen that, when $E_A \geq 7.4\ k_BT$ for $C_p = 20$ pN/nm or when $E_A \geq 9.1\ k_BT$ for the extreme value of $C_p = 30$ pN/nm, $T_R \geq 10$ s. The so large values of T_R imply that, before the incorporation of the nucleotide paired with the last base 43 on the template, the disruption of the DNA:RNA hybrid and then the repositioning of the primer 3′ end rarely occur. Thus, we give a good explanation to the fact that only when all of the bases on the template region are paired with the primer to form the DNA:RNA duplex can the distortion or conformational transition of the pseudoknot III induce the unpairing of the DNA:RNA duplex and then repositioning of product 3′-end to the beginning of the template.

It is interesting to note here that, only a binding affinity of $E_A \leq 9\ k_BT$ between site A and the template can give a very long time $T_R \approx 10$ s. This affinity of 9 k_BT corresponds to an equilibrium dissociation constant of about 0.1 mM. In other words, if only the interaction of site A in TERT with RNA template exists in telomerase, the mean dissociation constant of telomerase RNA from TERT is in the order of 0.1 mM, implying a very weak interaction between the telomerase RNA and TERT. This is consistent with the experimental data, showing that by mutating CA15-16GU in the *T. thermophila* telomerase RNA, which defects severely the interaction between TERT and the telomerase RNA except the template region, only a low fraction of the mutant telomerase RNA (<10% of wild type) was detected to interact with TERT [61].

3.3.2. Effect of stem III pseudoknot

In this section, we use Eq. (7) to study the effect of stem III on the repeat addition processivity. In the case that the stem III pseudoknot is unable to fold (e.g., using a mutant CCCC:UUUU instead of the wild-type pseudoknot stem AACC:UUGG), we always have $E_{III} = 0$ in our model. After the incorporation of dGTP paired with the last base 43, we have $E_A = 0$. Then, using Eq. (7) we calculate $T_R^{(MT)}/T_R^{(WT)}$ versus C_p, where $T_R^{(MT)}$ represents T_R in the case of mutant CCCC:UUUU while $T_R^{(WT)}$ represents T_R in the case of wild-type AACC:UUGG. The results are shown in Fig. 9a. It is seen that the ratio $T_R^{(MT)}/T_R^{(WT)}$ changes little

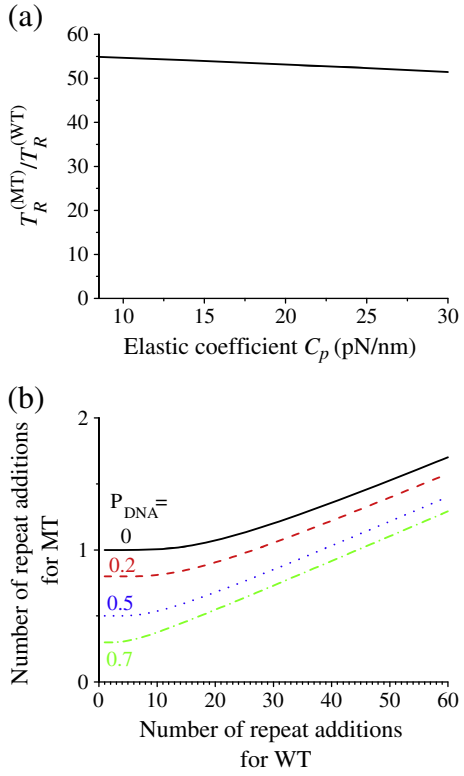

Fig. 9. Results for the effect of stem III pseudoknot on the repeat addition processivity. (a) Ratio of time $T_R^{(MT)}$ without the effect of stem III pseudoknot for a mutant (MT) telomerase versus time $T_R^{(WT)}$ with the effect of stem III pseudoknot for the wild-type (WT) telomerase as a function of the elastic coefficient C_p, where $T_R^{(MT)}$ and $T_R^{(WT)}$ denote the time taken to disrupt the DNA:RNA hybrid and then reposition the primer 3′ end to the beginning of the template after the incorporation of dGTP paired with the last base C43 on the template. (b) Number of repeat addition rounds without the effect of stem III pseudoknot for a mutant (MT) telomerase versus that with the effect of stem III pseudoknot for the wild-type (WT) telomerase.

with the variation of C_p: in the range of $C_p = 8.5$–30 pN/nm, $T_R^{(MT)}/T_R^{(WT)} \approx 53$.

Since during the time period of T_R no interaction exists between the RT domain and the template, the RT domain would show a much larger probability to deviate from the DNA:RNA hybrid or the template by a sufficient distance along the direction perpendicular to the central axis of the hybrid than that during other periods when the RT domain binds to the template region. In fact, using Eq. (5), it is obtained that the addition of $E_A = 9\ k_BT$ to U_0 reduces the time for the RT domain to deviate from the template along the direction perpendicular to the central axis of the DNA:RNA hybrid by about 10,000-fold. Thus, the above results imply that, after the incorporation of one repeat, the RT would show a much larger probability to deviate from the template of the mutant telomerase RNA than from the template of the wild-type telomerase RNA, i.e., the termination probability of the telomerase activity for the mutant telomerase RNA is much larger than that for the wild-type one, as just mentioned above. If we denote $P^{(WT)}$ as the probability for the RT domain to deviate from the template of the wild-type telomerase RNA during the time period of $T_R^{(WT)}$, then the probability for the RT domain to deviate from the template of the mutant telomerase RNA during the time period of $T_R^{(MT)}$ is

$$P^{(MT)} = 1 - \left(1 - P^{(WT)}\right)^F, \tag{8a}$$

$$F = \frac{T_R^{(MT)}}{T_R^{(WT)}}. \tag{8b}$$

The mean number of repeat addition rounds, R, is related to the probability P for the RT domain to deviate from the template during the time period of T_R by equation, $R=(1-P_{DNA})P^{-1}$,[5] where P_{DNA} is the dissociation probability of the DNA primer from the telomerase, which is independent of the time period T_R (see Section 3.2) and thus is considered to be the same for both the mutant and wild-type cases. From Eqs. (8a) and (8b) we have

$$R^{(MT)} = (1-P_{DNA})\left[1-\left(1-\frac{1-P_{DNA}}{R^{(WT)}}\right)^{F}\right]^{-1}. \quad (9)$$

Using Eq. (9) and with $F=T_R^{(MT)}/T_R^{(WT)}\approx 53$, the calculated results of $R^{(MT)}$ versus $R^{(WT)}$ for different values of P_{DNA} are shown in Fig. 9b. It is seen that the repeat addition processivity for the mutant telomerase RNA is reduced significantly as compared to the wild-type one. Since stem III pseudoknot for the wild-type telomerase RNA is unfolded by the moving of stem IV towards the active site, it is thus deduced that the repeat addition processivity is significantly stimulated by stem IV cooperated with stem III pseudoknot, which is consistent with prior experimental results [20–22].

On the other hand, if stem III pseudoknot is unable to unfold (e.g., using a stable mutant stem CCCCCC:GGGGGG instead of the wild-type pseudoknot stem AACC:UUGG), the stem IV cannot reach the polymerase active site when it is positioned beyond the last base 43 on the template upon the binding of dGTP. Then, we have the same result as for the case that the stem III pseudoknot is unable to fold (Fig. 9). Thus, the repeat addition processivity is also reduced greatly.

From above results, it is thus concluded that the transitions between folding and unfolding of stem III pseudoknot play an important role in facilitating repeat addition processivity.

3.3.3. Effect of dGTP versus that of dTTP on stimulation of repeat addition

Previous experiment showed that *Tetrahymena* telomerase has a K_m for dGTP incorporation that is about 10-fold lower than the K_m for incorporation of dTTP [62]. Then, it can be deduced that dGTP-binding rate is 10-fold higher than dTTP-binding rate. This implies $T^{(dTTP)}\approx 10T^{(dGTP)}$ for the same concentration of dGTP and dTTP, where $T^{(dTTP)}$ and $T^{(dGTP)}$ represent, respectively, the dTTP-binding time and the dGTP-binding time to the active site after the incorporation of the nucleotide paired with the last base 43. Similar to Eq. (9), we have the following relation

$$R^{(dTTP)} = (1-P_{DNA})\left[1-\left(1-\frac{1-P_{DNA}}{R^{(dGTP)}}\right)^{E}\right]^{-1}, \quad (10)$$

where $E=T^{(dTTP)}/T^{(dGTP)}=10$. $R^{(dTTP)}$ and $R^{(dGTP)}$ represent the mean number of repeat addition rounds stimulated by dTTP and that by dGTP, respectively, with the same nucleotide concentration. Using Eq. (10), the calculated results of $R^{(dTTP)}$ versus $R^{(dGTP)}$ are shown in Fig. 10. It is evident that dGTP has a much higher effect than dTTP on the stimulation of the repeat addition processivity.

3.3.4. Mutant templates in telomerase RNA

In this section, we use Eqs. (7) and (9) to study the effect of mutant templates on the repeat addition processivity.

First, we study the effect of the extended template. As in Hardy et al. [63], consider a mutant 7-nt T_2G_5 repeat instead of the wild-type 6-nt T_2G_4 repeat. For this case, after the incorporation of the nucleotide paired with the last base on the template, the potential depth E_H is calculated to be 11.2 kcal/mol (~18.9 k_BT) by using parameters for the nearest-neighboring thermodynamic model for DNA:RNA duplex stabilities [56]. The free-energy change required to unfold pseudoknot III is still approximately equal to $E_{III}=4.2\ k_BT$.

[5] In the previous work [34], the dissociation probability of DNA primer from the telomerase was taken to be $P_{DNA}=0$.

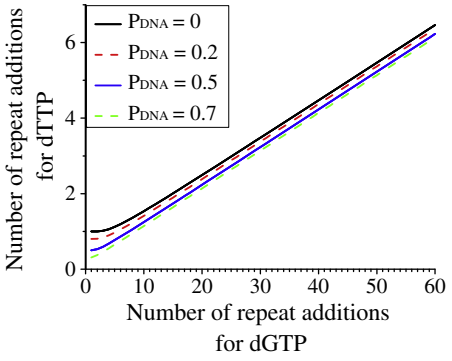

Fig. 10. Results for the effect of dGTP versus that of dTTP on stimulation of repeat addition processivity. Number of repeat addition rounds stimulated by dTTP versus that by dGTP for the same concentration of dTTP and dGTP. Curves from upper to lower correspond to $P_{DNA}=0$, 0.2, 0.5 and 0.7.

Thus, using Eq. (7) and with $E_A=0$, we calculated $T_R^{(MT)}/T_R^{(WT)}$ versus C_p, where $X=7p$ for the mutant 7-nt T_2G_5 repeat while $X=6p$ for the wild-type 6-nt T_2G_4 repeat. The results show that, in the range of $C_p=8.5$–30 pN/nm, $T_R^{(MT)}/T_R^{(WT)}$is in the range of 26–15. Using Eq. (9), the calculated results of $R^{(MT)}$ versus $R^{(WT)}$ for different values of C_p are shown in Fig. 11. It is seen that the repeat addition processivity is reduced greatly as compared to the wild-type template, which is consistent with the experimental data [63]. Similarly, for the repeat having more than 7 bases (e.g., T_2G_6), our results show further reduction of the repeat addition processivity (data not shown).

Then, we study the effect of the shortened template. Consider a 5-nt T_2G_3 repeat. After the incorporation of the nucleotide paired with the last base on the template, the potential depth of E_H becomes 11.8 k_BT and the free-energy change required to unfold pseudoknot III is $E_{III}=3.2\ k_BT$. Thus, using Eq. (7) and with $E_A=0$, we calculate $T_R^{(MT)}/T_R^{(WT)}$ versus C_p, where $X=5p$ for the mutant 5-nt T_2G_3 repeat while $X=6p$ for the wild-type 6-nt T_2G_4 repeat. The results show that, in the range of $C_p=8.5$–30 pN/nm, $T_R^{(MT)}/T_R^{(WT)}$ is in the range of 0.2–0.35. This gives a smaller probability for the RT domain to deviate from the DNA:RNA hybrid along the direction perpendicular to the central axis of the hybrid than the wild-type case. However, it is important to note here that, since the anchor site has specificity for telomeric sequence or a G-rich sequence, the primer of T_2G_3 repeat has a smaller binding affinity for the anchor site than the wild-type T_2G_4 repeat due to the less amount of G for the former than for the latter. Thus, the primer of T_2G_3 repeat has a higher probability to dissociate from TERT than the wild type. The two opposite effects can thus result in that the repeat addition processivity for the T_2G_3 repeat is slightly smaller than the wild-type repeat, which is consistent with the experimental data [63].

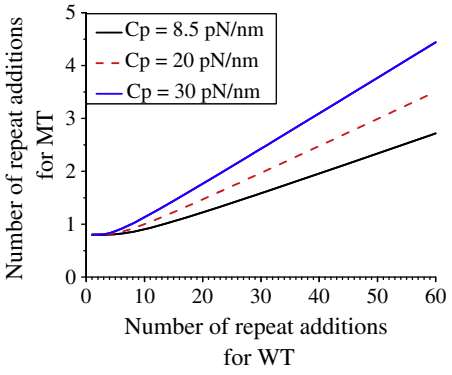

Fig. 11. Results for the effect of mutant (MT) templates on the repeat addition processivity. Number of repeat addition rounds for mutant templates versus that for the wild-type (WT) template. $P_{DNA}=0.2$.

It is important to note here that, in the above calculation for the effect of mutant templates, for simplicity, we only considered the effect of the base-pairing free energy due to mutant bases on the template. The mutant template may also have effects on the interaction of the anchor site with telomerase products, on the interaction of PAS with the primer and on the interaction of binding site *A* with the template. It is evident that both the reduction of the anchor site interacting with the primer and the reduction of the PAS interacting with the primer reduce the processivity. As discussed in Section 2.1.1, the reduction of the affinity of site *A* for the template may reduce the nucleotide-incorporation fidelity. As shown in Section 3.3.1 (see also Fig. 8), the reduction of the affinity of site *A* for the template increases the probability of premature repositioning of the active site to the beginning of the template, where the primer is relatively easily dissociated (see Section 3.2.2), inducing premature dissociations. Thus, the mutant template may affect both the fidelity and the processivity, as demonstrated by experiments of Gilley et al. [64] and Drosopoulos et al. [65].

3.3.5. Effect of external force on stimulation of repeat addition

In this section, we present some predicted results for the case that an external force, F_{ext}, acts on the RT domain containing the binding site *A* and active site. The force points to the direction that resists the RT domain moving towards the TEN and TRBD domains. The experiment for this case can be realized by using the optical trapping method with the movable micro-bead connecting to the RT domain while keeping the TEN and TRBD domains fixed.

Using Eqs. (S2), (S3a) and (S3b) (see Section S3 in the Appendix), the calculated results of $R^{(F_{ext})}$ versus $R^{(0)}$ for different values of F_{ext} are shown in Fig. 12, where $R^{(F_{ext})}$ and $R^{(0)}$ represent the mean number of repeat addition rounds with and without the effect of the external force F_{ext}, respectively. It is seen that the external force F_{ext} reduces the repeat addition processivity. The larger the external force is, the more reduction the repeat addition processivity is. This is an interesting result for our model, because, although the external force facilitates the movement of the RT domain relative to the TEN and TRBD domains during the processive nucleotide addition, it reduces the repeat addition processivity. The future experiment is hoped to test the prediction.

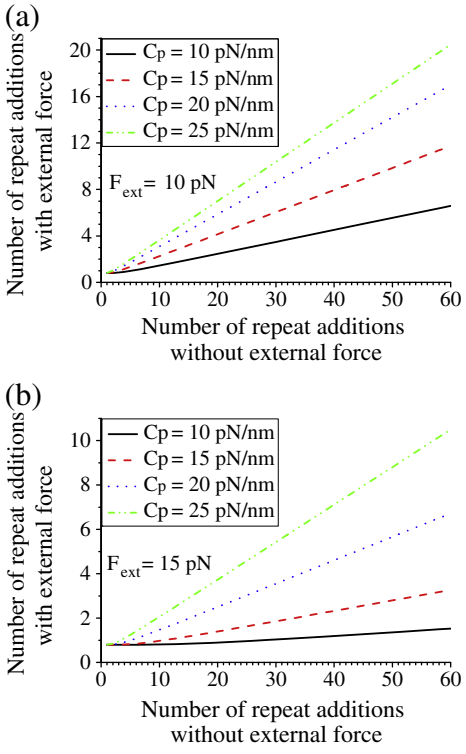

Fig. 12. Results for the effect of the external force F_{ext} on the repeat addition processivity. Number of repeat addition rounds with the external force versus that without the external force for the wild-type telomerase RNA, with $P_{DNA} = 0.2$. (a) $F_{ext} = 10$ pN. (b) $F_{ext} = 15$ pN.

4. Summary

In this work, based on available experimental data, we modify the model proposed before for nucleotide and repeat addition processivities by the recombinant telomerase. Based on the modified model, some characteristics for the recombinant *Tetrahymena* telomerase are quantitatively studied.

In Section 3.1, using some of experimental data for the minimal lengths required for primers to be extended by the *Tetrahymena* telomerase [46] and base-paring free energy, the value of the binding affinity of PAS to the primer is estimated. Using the estimated value, the obtained results are also consistent with other experimental data in Ref. [46].

In Section 3.2.1, we study the dissociation probability of the primer from telomerase during the time period of the transition from the previous round of repeat addition to the next one. The period can be considered to be composed of two sub-periods: one sub-period from the moment of the completion of the incorporation of dGTP paired with the last base C43 on the template through the moment when one repeat of DNA:RNA hybrid and the interaction of PAS with the primer are disrupted; the other one from the moment when the repeat of DNA:RNA hybrid and the interaction of PAS with the primer are disrupted through the moment when the binding site *A* rebinds to the unpaired base C48, the PAS rebinds to the primer and the TTG:AAC hybrid forms. During the former sub-period, the interaction of the primer with telomerase is via three binding sites: the anchor site, PAS and base-pairing interaction. By solving the moving equation of the primer relative to the telomerase, Eq. (4), we obtain that the dissociation probability of the primer from the telomerase during the former sub-period is negligibly small. During the latter sub-period, the interaction of the primer with the telomerase is only via the anchor site. The results show that the primer has a very small probability to detach from the telomerase during this sub-period. Taken together, we conclude that, during the period of the transition from previous round of repeat addition to the next one, the dissociation probability of the primer from the telomerase is very small.

Using the same procedure, we also study in Section 3.2.1 the dissociation probability of a primer with the minimal length that can be extended by the *Tetrahymena* telomerase. For this case, no interaction exists between the primer and the anchor site. We obtain that, during the period of the transition from the first round of repeat addition to the second one, only low fraction of the primers are dissociated from the telomerase. After transition to the second round of repeat addition, since the extended primer can interact with the anchor site, the primer would show much lower probability to dissociate from the telomerase. Thus, the minimal lengths required for primers to be extended with the telomerase by multiple repeats can be approximately said to be the same as those by a single nucleotide, which is consistent with the experimental data [46].

In Section 3.2.2, by solving the moving equation of the primer relative to the telomerase, Eq. (4), we calculate the dissociation probability of the primer during the period of nucleotide addition. During this period, the interaction of the primer with telomerase is via three binding sites: the anchor site, PAS and base-pairing interaction. The results show that the dissociation probability decrease as the number of incorporated nucleotides is increased, because the base-paring energy is increased. The dissociation of the primer from the telomerase occurs mainly during the incorporation of the 1st nucleotide. Particularly, in the absence of anchor site, a primer would show a very large probability to detach from the telomerase

during the incorporation of the 1st nucleotide. Thus, based on our model, the existence of anchor site in telomerase is more important to ensure the primer not to detach from the telomerase at the initiation of the nucleotide addition period than during the period of the transition from previous round of repeat addition to the next one. This is consistent with the inference from Baran et al. [46].

In Section 3.3.1, using Eq. (7) we obtain the mean time T_R taken to disrupt the DNA:RNA hybrid and then reposition the primer 3′ end to the beginning of the template after the incorporation of the nucleotide paired with the last base C43 on the template for the wild-type telomerase RNA. For this case, the binding affinity of site A for the template, $E_A = 0$. The obtained value of T_R is short so that it ensures the RT domain having a small probability to return to the equilibrium position relative to the TEN and TRBD domains without disruption of the hybrid, thus giving the high repeat addition processivity. Moreover, using Eq. (7) we obtain the mean time T_R before the incorporation of dGTP paired with the last base C43. For this case, due to $E_A \neq 0$, values of T_R become very large. The so large values of T_R imply that, before the incorporation of the nucleotide paired with the last base 43 on the template, the disruption of the DNA:RNA hybrid and the repositioning of the primer 3′ end rarely occur. Thus, this gives a good explanation to the fact that only when all of the bases on the template region are paired with the primer to form the DNA:RNA duplex can the unpairing of the DNA:RNA duplex and then repositioning of product 3′-end to the beginning of the template occur.

In Section 3.3.2, using Eq. (7) we obtain the mean time $T_R^{(MT)}$ for the case of mutant stem III pseudoknot that is unable to fold. From the comparison of $T_R^{(MT)}$ with $T_R^{(WT)}$ for the case of wild-type stem III pseudoknot, using Eqs. (8a), (8b) and (9) we obtain the relation of the mean number of repeat addition rounds, $R^{(MT)}$, for the mutant stem III pseudoknot versus that $R^{(WT)}$ for the wild-type stem III pseudoknot (Fig. 9b). The repeat addition processivity for the mutant telomerase RNA is reduced significantly as compared to the wild-type one. Since stem III pseudoknot for the wild-type telomerase is unfolded by the moving of stem IV towards the active site, it is thus deduced that the repeat addition processivity is significantly stimulated by stem IV cooperated with stem III pseudoknot, which is consistent with available experimental data [20–22].

In Section 3.3.3, using Eq. (10) we obtain the relation of the mean number of repeat addition rounds, $R^{(dTTP)}$, stimulated by dTTP versus that $R^{(dGTP)}$ stimulated by dGTP (Fig. 10). It is evident that dGTP has a much higher effect than dTTP on the stimulation of the repeat addition processivity, which is consistent with the experimental data.

In Section 3.3.4, considering only the effect of the base-pairing free energy due to mutant bases on the template, using Eq. (7) we obtain the mean time $T_R^{(MT)}$ for some mutant templates. From the comparison of $T_R^{(MT)}$ with $T_R^{(WT)}$ for the wild-type template, using Eqs. (8a), (8b) and (9) we obtain the relation of the mean number of repeat addition rounds, $R^{(MT)}$, for the mutant template versus that $R^{(WT)}$ for the wild-type template (Fig. 11). The results are consistent with the experimental data of Hardy et al. [63].

In Section 3.3.5, we study the effect of an external force on repeat addition processivity. The results showed that the external force, which resists the RT domain moving towards the TEN and TRBD domains, reduces the repeat addition processivity. The larger the external force is, the more reduction the repeat addition processivity is. This is an interesting result for our model, because, although the external force facilitates the movement of the RT domain relative to the TEN and TRBD domains during the processive nucleotide addition, it reduces the repeat addition processivity.

In conclusion, we present a translocation model for processive nucleotide and repeat additions by the recombinant telomerase via modification of the previous one. The following factors, which have significant effects on the dynamics of nucleotide and repeat additions but have been overlooked or not been considered in the previous one, are incorporated into the modified model and are considered in the mathematical studies of the dynamics: (i) the presence of primer alignment site (PAS) [46–48], (ii) the dissociation of primer, (iii) the non-zero values of the elastic force between movable RT domain and other domains of TERT, as well as (iv) the presence of the affinity between TEN and RT domains [50], etc. Based on the modified model, the dynamics of *Tetrahymena* telomerase is studied quantitatively. The theoretical results are in agreement with the available experimental data. Moreover, some predicted results are presented.

Acknowledgments

The author thanks Dr. H. Manor for helpful discussions. This work is supported by the National Natural Science Foundation of China (grant no. 10974248).

Appendix A. Supplementary data

Supplementary data to this article can be found online at doi:10.1016/j.bpc.2010.10.007.

References

[1] C.W. Greider, E.H. Blackburn, Identification of a specific telomere terminal transferase activity in *Tetrahymena* extracts, Cell 43 (1985) 405–413.
[2] T.R. Cech, Beginning to understand the end of the chromosome, Cell 116 (2004) 273–279.
[3] K. Collins, The biogenesis and regulation of telomerase holoenzymes, Nat. Rev. Mol. Cell Biol. 7 (2006) 484–494.
[4] N.F. Lue, Adding to the ends: what makes telomerase processive and how important is it? Bioessays 26 (2004) 955–962.
[5] L. Harrington, Biochemical aspects of telomerase function, Cancer Lett. 194 (2003) 139–154.
[6] K.L. Witkin, K. Collins, Holoenzyme proteins required for the physiological assembly and activity of telomerase, Genes Dev. 18 (2004) 1107–1118.
[7] D. Shippen-Lentz, E.H. Blackburn, Functional evidence for an RNA template in telomerase, Science 247 (1990) 546–552.
[8] D.P. Romero, E.H. Blackburn, A conserved secondary structure for telomerase RNA, Cell 67 (1991) 343–353.
[9] J. Lingner, L.L. Hendrick, T.R. Cech, Telomerase RNAs of different ciliates have a common secondary structure and a permuted template, Genes Dev. 8 (1994) 1984–1998.
[10] M. McCormick-Graham, D.P. Romero, Ciliate telomerase RNA structural features, Nucleic Acids Res. 23 (1995) 1091–1097.
[11] M. McCormick-Graham, D.P. Romero, A single telomerase RNA is sufficient for the synthesis of variable telomeric DNA repeats in ciliates of the genus *Paramecium*, Mol. Cell. Biol. 16 (1996) 1871–1879.
[12] M.S. Singer, D.E. Gottschling, *TLC1*: template RNA component of *Saccharomyces cerevisiae* telomerase, Science 266 (1994) 404–409.
[13] M.J. McEachern, E.H. Blackburn, Runaway telomere elongation caused by telomerase RNA gene mutations, Nature 376 (1995) 403–409.
[14] M.A. Blasco, W. Funk, B. Villeponteau, C.W. Greider, Functional characterization and developmental regulation of mouse telomerase RNA, Science 269 (1995) 1267–1270.
[15] J.L. Chen, M.A. Blasco, C.W. Greider, Secondary structure of vertebrate telomerase RNA, Cell 100 (2000) 503–514.
[16] J. Feng, W.D. Funk, S.-S. Wang, S.L. Weinrich, A.A. Avilion, C.-P. Chiu, R.R. Adams, E. Chang, R.C. Allsopp, J. Yu, S. Le, M.D. West, C.B. Harley, W.H. Andrews, C.W. Greider, B. Villeponteau, The RNA component of human telomerase, Science 269 (1995) 1236–1241.
[17] C.W. Greider, E.H. Blackburn, A telomeric sequence in the RNA of *Tetrahymena* telomerase required for telomere repeat synthesis, Nature 337 (1989) 331–337.
[18] C.K. Lai, M.C. Miller, K. Collins, Template boundary definition in *Tetrahymena* telomerase, Genes Dev. 16 (2002) 415–420.
[19] M.C. Miller, K. Collins, Telomerase recognizes its template by using an adjacent RNA motif, Proc. Natl Acad. Sci. USA 99 (2002) 6585–6590.
[20] C.K. Lai, M.C. Miller, K. Collins, Roles for RNA in telomerase nucleotide and repeat addition processivity, Mol. Cell 11 (2003) 1673–1683.
[21] D.X. Mason, E. Goneska, C.W. Greider, Stem-loop IV of *Tetrahymena* telomerase RNA stimulates processivity in *trans*, Mol. Cell. Biol. 23 (2003) 5606–5613.
[22] J.M. Sperger, T.R. Cech, A stem-loop of Tetrahymena telomerase RNA distant from the template potentiates RNA folding and telomerase activity, Biochemistry 40 (2001) 7005–7016.
[23] J. Lingner, T.R. Hughes, A. Shevchenko, M. Mann, V. Lundblad, T.R. Cech, Reverse transcriptase motifs in the catalytic subunit of telomerase, Science 276 (1997) 561–567.
[24] C. Kelleher, M.T. Teixeira, K. Förstemann, J. Lingner, Telomerase: biochemical considerations for enzyme and substrate, Trends Biochem. Sci. 27 (2002) 572–579.

[25] A.J. Gillis, A.P. Schuller, E. Skordalakes, Structure of the *Tribolium castaneum* telomerase catalytic subunit TERT, Nature 455 (2008) 633–637.
[26] R. Prathapam, K.L. Witkin, C.M. O'Connor, K. Collins, A telomerase holoenzyme protein enhances telomerase RNA assembly with telom erase reverse transcriptase, Nat. Struct. Mol. Biol. 12 (2005) 252–257.
[27] C.M. O'Connor, K. Collins, A novel RNA binding domain in tetrahymena telomerase p65 initiates hierarchical assembly of telomerase holoenzyme, Mol. Cell. Biol. 26 (2006) 2029–2036.
[28] M.D. Stone, M. Mihalusova, C.M. O'Connor, R. Prathapam, K. Collins, X. Zhuang, Stepwise protein-mediated RNA folding directs assembly of telomerase ribonucleoprotein, Nature 446 (2007) 458–461.
[29] C.W. Greider, Telomerase is processive, Mol. Cell. Biol. 10 (1991) 4572–4580.
[30] G.B. Morin, The human telomere terminal transferase enzyme is a ribonucleoprotein that synthesizes TTAGGG repeats, Cell 59 (1989) 521–529.
[31] S.L. Weinrich, R. Pruzan, L. Ma, M. Ouellette, V.M. Tesmer, S.E. Holt, A.G. Bodnar, S. Lichtsteiner, N.W. Kim, J.B. Trager, R.D. Taylor, R. Carlos, W.H. Andrews, W.E. Wright, J.W. Shay, C.B. Harley, G.B. Morin, Reconstitution of human telomerase with the template RNA component hTR and the catalytic protein subunit hTRT, Nat. Genet. 17 (1997) 498–502.
[32] L. Harrington, W. Zhou, T. McPhail, R. Oulton, D.S.K. Yeung, V. Mar, M.B. Bass, M.O. Robinson, Human telomerase contains evolutionarily conserved catalytic and structural subunits, Genes Dev. 11 (1997) 3109–3115.
[33] K. Collins, L. Gandhi, The reverse transcriptase component of the *Tetrahymena* telomerase ribonucleoprotein complex, Proc. Natl Acad. Sci. USA 95 (1998) 8485–8490.
[34] P. Xie, A possible mechanism of processive nucleotide and repeat additions by the telomerase, BioSystems 97 (2009) 168–178.
[35] P. Xie, Model for forward polymerization and switching transition between polymerase and exonuclease sites by DNA polymerase molecular motors, Arch. Biochem. Biophys. 457 (2007) 73–84.
[36] P. Xie, A polymerase-site-jumping model for strand transfer during DNA synthesis by reverse transcriptase, Virus Res. 144 (2009) 65–73.
[37] S. Doublie, S. Tabor, A.M. Long, C.C. Richardson, T. Ellenberger, Crystal structure of a bacteriophage T7 DNA replication complex at 2.2 Å resolution, Nature 391 (1998) 251–258.
[38] S. Doublie, T. Ellenberger, The mechanism of action of T7 DNA polymerase, Curr. Opin. Struct. Biol. 8 (1998) 704–712.
[39] H. Huang, R. Chopra, G.L. Verdine, S.C. Harrison, Structure of a covalently trapped catalytic complex of HIV-1 reverse transcriptase: implications for drug resistance, Science 282 (1998) 1669–1675.
[40] Y.W. Yin, T.A. Steitz, The structural mechanism of translocation and helicase activity in T7 RNA polymerase, Cell 116 (2004) 393–404.
[41] D. Temiakov, V. Patlan, M. Anikin, W.T. McAllister, S. Yokoyama, D.G. Vassylyev, Structural basis for substrate selection by T7 RNA polymerase, Cell 116 (2004) 381–391.
[42] A.R. Robart, C.M. O'Connor, K. Collins, Ciliate telomerase RNA loop IV nucleotides promote hierarchical RNP assembly and holoenzyme stability, RNA 16 (2007) 563–571.
[43] S. Rouda, E. Skordalakes, Structure of the RNA-binding domain of telomerase: implications for RNA recognition and binding, Structure 15 (2007) 1403–1412.
[44] G.B. Morin, Recognition of a chromosome truncation site associated with alpha-thalassaemia by human telomerase, Nature 353 (1991) 454–456.
[45] P.W. Hammond, T.N. Lively, T.R. Cech, The anchor site of telomerase from *Euplotes aediculatus* revealed by photo-cross-linking to single- and double-stranded DNA primers, Mol. Cell. Biol. 17 (1997) 296–308.
[46] N. Baran, Y. Haviv, B. Paul, H. Manor, Studies on the minimal lengths required for DNA primers to be extended by the *Tetrahymena* telomerase: implications for primer positioning by the enzyme, Nucleic Acids Res. 30 (2002) 5570–5578.
[47] E. Romi, N. Baran, M. Gantman, M. Shmoish, B. Min, K. Collins, H. Manor, High-resolution physical and functional mapping of the template adjacent DNA binding site in catalytically active telomerase, Proc. Natl Acad. Sci. USA 104 (2007) 8791–8796.
[48] S.A. Jacobs, E.R. Podell, T.R. Cech, Crystal structure of the essential N-terminal domain of telomerase reverse transcriptase, Nat. Struct. Mol. Biol. 13 (2006) 218–225.
[49] S.N. Finger, T.M. Bryan, Multiple DNA-binding sites in *Tetrahymena* telomerase, Nucleic Acids Res. 36 (2008) 1260–1272.
[50] A. Zaug, E.R. Podell, T.R. Cech, Mutation in TERT separates processivity from anchor-site function, Nat. Struct. Mol. Biol. 15 (2008) 870–872.
[51] K. Collins, C.W. Greider, *Tetrahymena* telomerase catalyzes nucleolytic cleavage and nonprocessive elongation, Genes Dev. 7 (1993) 1364–1376.
[52] M.J. Donlin, S.S. Patel, K.A. Johnson, Kinetic partitioning between the exonuclease and polymerase sites in DNA error correction, Biochemistry 30 (1991) 538–546.
[53] M.J. Thomas, A.A. Platas, D.K. Hawley, Transcriptional fidelity and proofreading by RNA polymerase II, Cell 93 (1998) 627–637.
[54] P.W. Hammond, T.R. Cech, *Euplotes* telomerase: evidence for limited base-pairing during primer elongation and dGTP as an effector of translocation, Biochemistry 37 (1998) 5162–5172.
[55] K. Forstemann, J. Lingner, Telomerase limits the extent of base pairing between template RNA and telomeric DNA, EMBO Rep. 6 (2005) 361–366.
[56] P. Wu, S. Nakano, N. Sugimoto, Temperature dependence of thermodynamic properties for DNA/DNA and RNA/DNA duplex formation, Eur. J. Biochem. 269 (2002) 2821–2830.
[57] Z. Bu, R. Biehl, M. Monkenbusch, D. Richter, D.J.E. Callaway, Coupled protein domain motion in *Taq* polymerase revealed by neutron spin-echo spectroscopy, Proc. Natl Acad. Sci. USA 102 (2005) 17,646–17,651.
[58] G. Zaccai, How soft is a protein? A protein dynamics force constant measured by neutron scattering, Science 288 (2000) 1604–1607.
[59] S.M. Freier, R. Kierzek, J.A. Jaeger, N. Sugimoto, M.H. Caruthers, T. Neilson, D.H. Tuener, Improved free-energy parameters for predictions of RNA duplex stability, Proc. Natl Acad. Sci. USA 83 (1986) 9373–9377.
[60] G. Wallweber, S. Gryaznov, K. Pongracz, R. Pruzan, Interaction of human telomerase with its primer substrate, Biochemistry 42 (2003) 589–600.
[61] J.D. Licht, K. Collins, Telomerase RNA function in recombinant *Tetrahymena* telomerase, Genes Dev. 13 (1999) 1116–1125.
[62] K. Collins, C.W. Greider, Utilization of ribonucleotides and RNA primers by *Tetrahymena* telomerase, EMBO J. 14 (1995) 5422–5432.
[63] C.D. Hardy, C.S. Schultz, K. Collins, Requirements for the dGTP-dependent repeat addition processivity of recombinant *Tetrahymena* telomerase, J. Biol. Chem. 276 (2001) 4863–4871.
[64] D. Gilley, M.S. Lee, E.H. Blackburn, Altering specific telomerase RNA template residues affects active site function, Genes Dev. 9 (1995) 2214–2226.
[65] W.C. Drosopoulos, R. DiRenzo, V.R. Prasad, Human telomerase RNA template sequence is a determinant of telomere repeat extension rate, J. Biol. Chem. 280 (2005) 32,801–32,810.
[66] C.W. Gardiner, Handbook of Stochastic Methods for Physics, Chemistry and the Natural Sciences, Springer-Verlag, Berlin, 1983.